

The no-hair theorems at work in M87*

LORENZO IORIO¹

¹Ministero dell' Istruzione e del Merito. Viale Unità di Italia 68, I-70125, Bari (BA), Italy

Abstract

Recently, a perturbative calculation to the first post-Newtonian order has shown that the analytically worked out Lense-Thirring precession of the orbital angular momentum of a test particle following a circular path around a massive spinning primary is able to explain the measured features of the jet precession of the supermassive black hole at the centre of the giant elliptical galaxy M87. It is shown that also the hole's mass quadrupole moment Q_2 , as given by the no-hair theorems, has a dynamical effect which cannot be neglected, as, instead, done so far in the literature. New allowed regions for the hole's dimensionless spin parameter a^* and the effective radius r_0 of the accretion disk, assumed tightly coupled with the jet, are obtained by including both the Lense-Thirring and the quadrupole effects in the dynamics of the effective test particle modeling the accretion disk. One obtains that, by numerically integrating the resulting averaged equations for the rates of change of the angles η and ϕ characterizing the orientation of the orbital angular momentum with $a^* = +0.98$ and $r_0 = 14.1$ gravitational radii, it is possible to reproduce, both quantitatively and qualitatively, the time series for them recently measured with the Very Long Baseline Interferometry technique. Instead, the resulting time series produced with $a^* = -0.95$ and $r_0 = 16$ gravitational radii turn out to be out of phase with respect to the observationally determined ones, while maintaining the same amplitudes.

Keywords: gravitation; galaxies:nuclei; galaxies:quasars:supermassive black holes; galaxies:jets

1. INTRODUCTION

It has recently been proven (Iorio 2024b) that a simple perturbative calculation to the first post-Newtonian (1pN) order of the Lense-Thirring (LT) effect on the orbit of a test particle moving about a massive spinning object is able to reproduce, both qualitatively and quantitatively, several features of the jet precession in the supermassive black hole (SMBH) M87* recently measured with the Very Long Baseline Interferometry (VLBI) technique (Cui et al. 2023). Aim of this paper is to show that, actually, also the mass quadrupole moment¹ of M87*, neglected so far in the literature, should be fully taken into account in the dynamics of the accretion disk, assumed tightly coupled with the jet (McKinney, Tchekhovskoy & Blandford 2013; Liska et al. 2018; Cui & Lin 2024). The imprints of the precession of the latter on the SMBH-accretion disk system was recently investigated in (Cui & Lin 2024). The introduction of the hole's quadrupole does not spoil the agreement between the perturbative analytical calculation and the characteristics measured in (Cui et al. 2023), yielding to different allowed regions for the hole's spin parameter and the radius of the effective circular orbit modeling the precessing disk. As a result, the celebrated "no-hair" (NH) theorems (Israel 1967; Carter 1971; Robinson 1975) receive a strong support.

According to the latter ones, the mass and the spin moments \mathcal{M}^ℓ and \mathcal{J}^ℓ of degree ℓ of a rotating BH (Bardeen 1970), whose external spacetime is described by the Kerr metric (Kerr 1963; Teukolsky 2015), are connected by the relation

$$\mathcal{M}^\ell + i \mathcal{J}^\ell = M \left(i \frac{J}{cM} \right)^\ell, \quad (1)$$

where $i := \sqrt{-1}$ is the imaginary unit, c is the speed of light, and M and J are the hole's mass and spin angular momentum, respectively. From Equation (1), it turns out that the odd mass moments and even spin moments are identically zero. In particular, the hole's mass moment \mathcal{M}^0 of degree $\ell = 0$ is its mass, while its spin dipole moment \mathcal{J} of degree $\ell = 1$ is its spin angular

¹ The possible impact of electric charge was recently investigated (Meng, Wang & Wei 2024) in the framework of the Kerr-Newman metric (Newman & Janis 1965; Newman et al. 1965) as well.

momentum. For a Kerr BH, it is (Shapiro & Teukolsky 1986)

$$J = \chi \frac{M^2 G}{c}, \quad |\chi| \leq 1, \quad (2)$$

where G is the Newtonian constant of gravitation. Furthermore, the mass quadrupole moment \mathcal{M}^2 of degree $\ell = 2$, renamed Q_2 , is

$$Q_2 = -\frac{J^2}{c^2 M}. \quad (3)$$

If $|\chi| > 1$, a naked singularity (Yodzis, Seifert & Müller Zum Hagen 1973; Shapiro & Teukolsky 1991) without a horizon would occur, implying the possibility of causality violations because of closed timelike curves. Although not yet proven, the cosmic censorship conjecture (Penrose 1999, 2002) states that naked singularities may not be formed via the gravitational collapse of a material body. The dimensionless parameter χ can also be viewed as the second characteristic length² $J/(cM)$ occurring in the Kerr metric (Kerr 1963; Teukolsky 2015) measured in units of the gravitational radius $R_g := GM/c^2$. In BH studies, χ is often denoted with a , which is the same symbol usually adopted in celestial mechanics and astrodynamics to denote the semimajor axis of a generally elliptical orbit of a test particle.

The organization of the paper is as follows. Section 2 offers a review of the perturbative analytical model of the LT and mass quadrupole effects, expressed in terms of the both the Keplerian orbital elements and in vectorial form, for a generic orientation of the primary's spin axis in space. In Section 3, the previous results are successfully applied to the measured precession of the jet of M87*, assumed strongly coupled with that of the accretion disk. Section 4 summarizes the findings and offers conclusions.

2. THE ANALYTICAL MODEL FOR THE ORBITAL PRECESSIONS

The inclination I and the longitude of the ascending node Ω define the orientation of the orbital plane in space. Their LT rates of change averaged over one orbital revolution and valid for an arbitrary orientation of the primary's spin axis $\hat{\mathbf{k}}$ turn out to be

$$j^{\text{LT}} = \frac{2GJ(\hat{\mathbf{k}} \cdot \hat{\mathbf{l}})}{c^2 a^3 (1 - e^2)^{3/2}}, \quad (4)$$

$$\dot{Q}^{\text{LT}} = \frac{2GJ \csc I (\hat{\mathbf{k}} \cdot \hat{\mathbf{m}})}{c^2 a^3 (1 - e^2)^{3/2}}, \quad (5)$$

where, for a Kerr BH, J is given by Equation (2). Furthermore, a and e are the orbit's semimajor axis and eccentricity, respectively. The unit vectors $\hat{\mathbf{l}}$ and $\hat{\mathbf{m}}$, which lie in the orbital plane and are mutually orthogonal, are defined as (Soffel 1989; Brumberg 1991; Soffel & Han 2019; Iorio 2024a)

$$\hat{\mathbf{l}} := \{\cos \Omega, \sin \Omega, 0\}, \quad (6)$$

$$\hat{\mathbf{m}} := \{-\cos I \sin \Omega, \cos I \cos \Omega, \sin I\}. \quad (7)$$

Equations (4)–(5) were worked out with a perturbative calculation to the 1pN order by means of the equations for the rates of change of the Keplerian orbital elements in Gaussian or Lagrange form (Soffel 1989; Brumberg 1991; Murray & Dermott 1999; Bertotti, Farinella & Vokrouhlický 2003; Roy 2005; Kopeikin, Efroimsky & Kaplan 2011; Poisson & Will 2014; Soffel & Han 2019; Iorio 2024a).

The mean rates of changes of the same orbital elements caused by the oblateness of a massive primary, valid for a generic orientation of $\hat{\mathbf{k}}$, can be calculated with the same approach obtaining (Iorio 2024a)

$$j^{Q_2} = -\frac{3}{2} n_K J_2 \left(\frac{R}{p}\right)^2 (\hat{\mathbf{k}} \cdot \hat{\mathbf{h}}) (\hat{\mathbf{k}} \cdot \hat{\mathbf{l}}), \quad (8)$$

² Sometimes, the symbol a is used for $J/(cM)$ itself, in which case it is dimensionally a length.

$$\dot{Q}^{Q_2} = -\frac{3}{2}n_K J_2 \csc I \left(\frac{R}{p}\right)^2 (\hat{\mathbf{k}} \cdot \hat{\mathbf{h}})(\hat{\mathbf{k}} \cdot \hat{\mathbf{m}}). \quad (9)$$

In Equations (8)–(9), $n_K := \sqrt{GM/a^3}$ is the Keplerian mean motion, $p := a(1 - e^2)$ is the semilatus rectum, the unit vector $\hat{\mathbf{h}}$, directed along the orbital angular momentum and orthogonal to both $\hat{\mathbf{l}}$ and $\hat{\mathbf{m}}$ in such a way that $\hat{\mathbf{l}} \times \hat{\mathbf{m}} = \hat{\mathbf{h}}$ holds, is defined as (Soffel 1989; Brumberg 1991; Soffel & Han 2019; Iorio 2024a)

$$\hat{\mathbf{h}} := \{\sin I \sin \Omega, -\sin I \cos \Omega, \cos I\}, \quad (10)$$

R is the equatorial radius of the primary, and J_2 is its dimensionless mass quadrupole moment. The latter one must be expressed in terms of its dimensional counterpart Q_2 having dimensions of a mass times a length squared as

$$J_2 := -\frac{Q_2}{MR^2}, \quad (11)$$

which, for a Kerr BH, is given by Equation (3).

The resulting NH orbital rates are

$$j^{\text{NH}} = j^{\text{LT}} + j^{Q_2}, \quad (12)$$

$$\dot{Q}^{\text{NH}} = \dot{Q}^{\text{LT}} + \dot{Q}^{Q_2}. \quad (13)$$

Equations (4)–(10) can be used to express the precession of the unit vector $\hat{\mathbf{h}}$ of the orbital angular momentum in a compact form as

$$\frac{d\hat{\mathbf{h}}}{dt} = \frac{\partial \hat{\mathbf{h}}}{\partial I} j^{\text{NH}} + \frac{\partial \hat{\mathbf{h}}}{\partial \Omega} \dot{Q}^{\text{NH}} = \boldsymbol{\Omega}_d^{\text{NH}} \times \hat{\mathbf{h}}. \quad (14)$$

In it, the precession velocity vector $\boldsymbol{\Omega}_d^{\text{NH}}$ is

$$\boldsymbol{\Omega}_d^{\text{NH}} = \boldsymbol{\Omega}_d^{\text{LT}} + \boldsymbol{\Omega}_d^{Q_2}, \quad (15)$$

where

$$\boldsymbol{\Omega}_d^{\text{LT}} = \frac{2GJ}{c^2 a^3 (1 - e^2)^{3/2}} \hat{\mathbf{k}}, \quad (16)$$

$$\boldsymbol{\Omega}_d^{Q_2} = -\frac{3}{2}n_K J_2 \left(\frac{R}{p}\right)^2 (\hat{\mathbf{k}} \cdot \hat{\mathbf{h}}) \hat{\mathbf{k}}. \quad (17)$$

From Equations (15)–(17), it can be noted that the orbital angular momentum precesses around the primary's spin axis. Such results are in agreement with (Barker & O'Connell 1974; Barker & O'Connell 1975), where the term accounting also for the simultaneous precession of the Laplace–Runge–Lenz vector (Goldstein 1980; Taff 1985), of no interest here, was included in the total precessional velocity.

3. APPLICATION TO M87*

In the following, the spin axis of M87* will be parameterized as

$$\hat{\mathbf{k}} = \{\sin \theta \sin \eta_p, -\sin \theta \cos \eta_p, \cos \theta\}, \quad (18)$$

where (Cui et al. 2023)

$$\theta = 17.21^\circ, \quad (19)$$

$$\eta_p = 288.47^\circ. \quad (20)$$

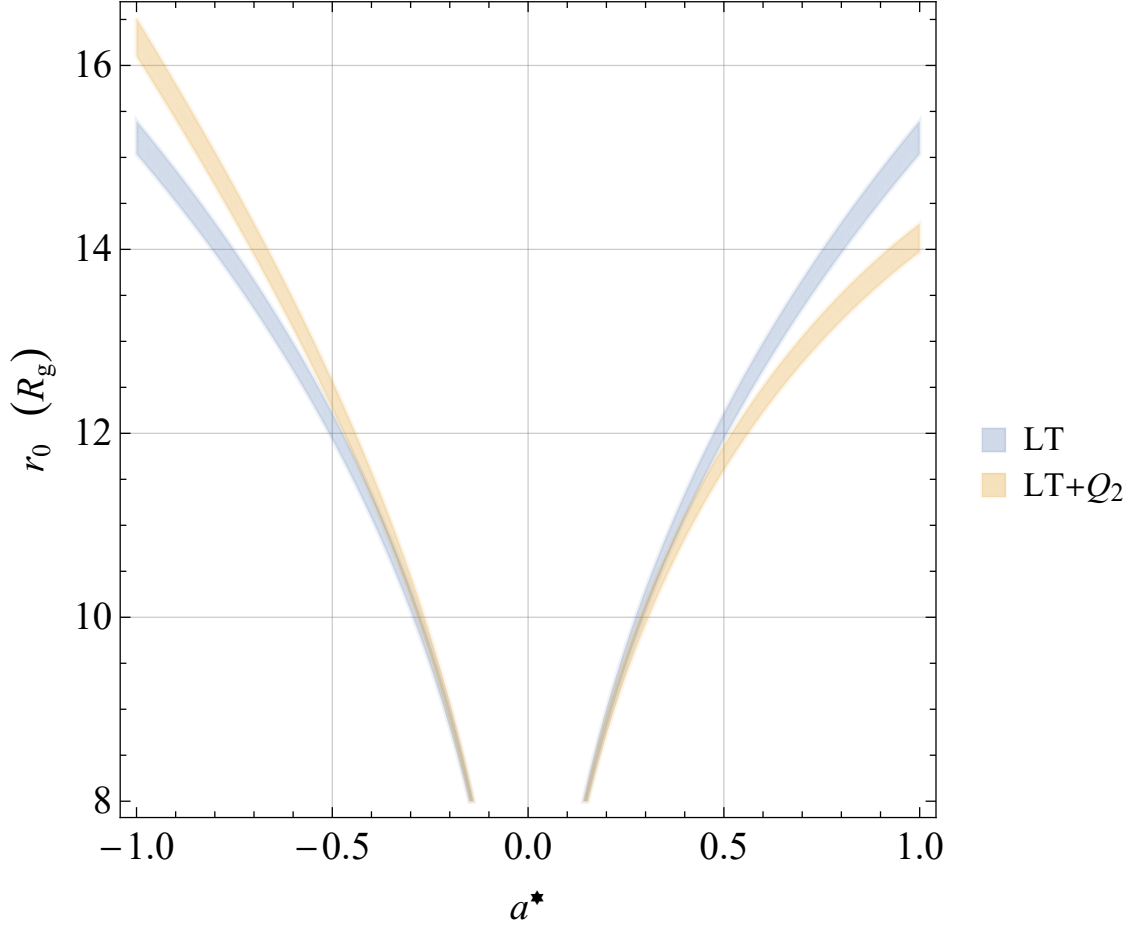


Figure 1. Entire allowed regions in the $\{a^*, r_0\}$ plane corresponding to the condition that the graphs of $|\Omega_d^{LT}(a^*, r_0)|$ and $|\Omega_d^{NH}(a^*, r_0)|$ remain confined between the upper and lower experimentally allowed values of $|\omega_p^{exp}|$, i.e., $0.54 \text{ rad yr}^{-1} \leq |\Omega_d^{LT}(a^*, r_0)|, |\Omega_d^{NH}(a^*, r_0)| \leq 0.58 \text{ rad yr}^{-1}$. The minimum value for r_0 has been taken from the largest expected radius of the TISCO orbit for $\psi_{jet} \simeq 0^\circ$, as per Figure 1 of (Al Zahrani 2024).

By considering the total NH precession velocity, given by Equations (15)–(17), as a function of a^* and the effective radius r_0 of the precessing accretion disk, it is possible to plot its absolute value by imposing the condition that its graph is comprised within the upper and lower measured values of the absolute value of the measured precession velocity (Cui et al. 2023)

$$|\omega_p^{exp}| = 0.56 \pm 0.02 \text{ rad yr}^{-1}, \quad (21)$$

i.e.,

$$0.54 \text{ rad yr}^{-1} \leq |\Omega_d^{NH}(a^*, r_0)| \leq 0.58 \text{ rad yr}^{-1}. \quad (22)$$

The sets of the values of a^* and r_0 satisfying the condition of Equation (22) form allowed regions in the $\{a^*, r_0\}$ plane depicted in pale yellow in Figure 1. In it, also the permitted regions obtained by considering solely the LT effect are shown in pale blue as well (Iorio 2024b). It turns out that both the LT and the LT + Q_2 regions overlap in the no-rotation limit $|a^*| \rightarrow 0$, as expected. Instead, they separate when the hole's spin parameter tends to unity. While both the allowed branches are equal and symmetric with respect to the $a^* = 0$ axis in the LT-only case, the inclusion of the SMBH's quadrupole breaks such a symmetry allowing for larger values of r_0 corresponding to the retrograde rotation of the hole ($a^* < 0$) with respect to the prograde case ($a^* > 0$). As a general feature, for prograde hole's rotation, Q_2 generally tends to shrink the disk (right branches), while the opposite occurs for retrograde hole's rotation (left branches) with respect to the LT-only scenario. The minimum physically admissible value for r_0 was taken from Figure 1 of (Al Zahrani 2024) which depicts the radius of the tilted³ innermost stable circular orbit (TISCO) for

³ The tilt is with respect to the hole's equator.

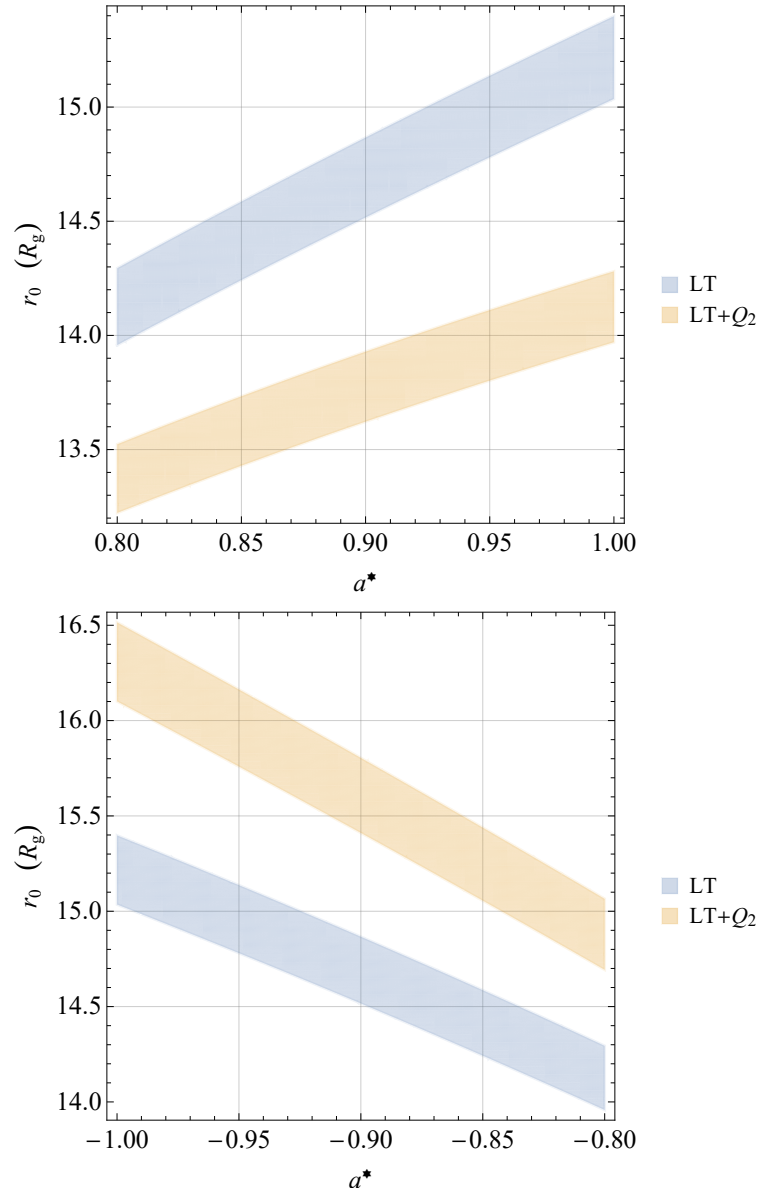


Figure 2. Insets of Figure 1 for positive (upper panel) and negative (lower panel) values of the SMBH’s spin parameter close to unity. The pale blue and pale yellow allowed regions correspond to the LT-only and LT + Q_2 cases, respectively.

different values of the spin–orbit tilt angle, called ψ_{jet} in (Cui et al. 2023) (see below for more on it). It turns out that, for slightly tilted orbits as in the case of M87* ($\psi_{\text{jet}}^{\text{M87*}} \approx 1.25^\circ$ (Cui et al. 2023)), the radius of the TISCO is

$$r_{\text{TISCO}} \approx 8R_g \quad (a^* \approx -1), \quad (23)$$

$$r_{\text{TISCO}} \approx 2R_g \quad (a^* \approx 1). \quad (24)$$

Figure 2 shows two insets of Figure 1 corresponding to $|a^*| \lesssim 1$, in agreement with most of the constraints on it existing in the literature (Kissler-Patig & Gebhardt 1998; Wang et al. 2008; Li et al. 2009; Doeleman et al. 2012; Feng & Wu 2017; Sob’yanin 2018; Nemmen 2019; Nokhrina et al. 2019; Garofalo 2020; Tamburini, Thidé & Della Valle 2020; Dokuchaev 2023). In such regimes, the impact of Q_2 appears quite evident with respect to the case in which only the LT effect is taken into account.

Numerically integrated NH time series of the time–dependent angles $\eta(t)$ and $\phi(t)$ determining the orientation of the disk’s orbital angular momentum in space can be produced; in the language of celestial mechanics and astrodynamics, they correspond

to the longitude of the ascending node Ω and the inclination I , respectively. Their signatures were theoretically obtained by simultaneously integrating the averaged equations for the rates of change of Equations (12)–(13) by adopting the values $a^* = +0.98, r_0 = 14.1 R_g$ and $a^* = -0.95, r_0 = 16 R_g$, contained in the pale yellow regions of the upper and lower panels of Figure 2, respectively. The time spans of the integration have the same length as in Extended Data Figure 4 of (Cui et al. 2023) for a better comparison with the latter ones. It turns out that the NH prograde signatures agree well with their measured counterparts of Figure 2 (b) and Extended Data Figure 4 of (Cui et al. 2023), both qualitatively and quantitatively. It is not the case for the NH retrograde signals which, if on the one hand, retain the same sizes of those in Figure 2 (b) and Extended Data Figure 4 of (Cui et al. 2023), on the other hand, are out of phase with respect to the latter ones.

As far as the spin–orbit tilt angle ψ_{jet} is concerned, both its theoretically predicted value and its temporal evolution, calculated by integrating Equations (12)–(13) as before, do not change with respect to their LT–only counterparts, shown in Figure 5 of (Iorio 2024b), which were already found to be in agreement with their measured values.

4. SUMMARY AND CONCLUSIONS

The no–hair theorems are fully at work in M87*. Indeed, it has been shown that not only the hole’s spin dipole moment J through the Lense–Thirring effect but also its mass quadrupole moment Q_2 , both calculated according to them, are able to explain the recently observed phenomenology of the jet precession of the supermassive black hole lurking at the centre of the galaxy M87. The inclusion of the precession induced by Q_2 , calculated perturbatively as the Lense–Thirring one, yields to a modification of the allowed regions in the parameter space spanned by the hole’s spin parameter a^* and the effective radius r_0 of the accretion disk, assumed tightly coupled with the jet, with respect to the Lense–Thirring only case. Indeed, while neglecting Q_2 one obtains two identical permitted branches in the $\{a^*, r_0\}$ plane which are symmetric with respect to the $a^* = 0$ axis, the introduction of the hole’s oblateness breaks such a symmetry since the allowed branch corresponding to retrograde hole’s rotation gives larger allowed values for r_0 with respect to the prograde one. Furthermore, the presence of Q_2 tends to shrink (enlarge) the disk for prograde (retrograde) rotation with respect to the scenario in which it is omitted. The simultaneous numerical integration of the averaged equations for the spin dipole and mass quadrupole rates of change of the angles determining the orientation of the disk’s orbital angular momentum with $a^* = 0.98$ and $r_0 = 14.1$ gravitational radii allows to reproduce all the qualitative and quantitative features of the corresponding measured time series. It is not so for negative values of the hole’s spin and the corresponding disk’s radii which return out of phase theoretical signatures with respect to the empirical ones, while maintaining the same amplitudes. Finally, the value of the spin–orbit tilt angle between the angular momenta of the hole and the disk remains unchanged, along with its constancy over time.

DATA AVAILABILITY

No new data were generated or analysed in support of this research.

CONFLICT OF INTEREST STATEMENT

I declare no conflicts of interest.

ACKNOWLEDGEMENTS

I am grateful to M. Zajaček and Cui Y. for useful information and explanations. I wish to thank also an anonymous referee for the appreciation paid to this work.

REFERENCES

- | | |
|--|--|
| <p>Al Zahrani A. M., 2024, Phys. Rev. D, 109, 024029</p> <p>Bardeen J. M., 1970, Nature, 226, 64</p> <p>Barker B. M., Oconnell R. F., 1974, Phys. Rev. D, 10, 1340</p> <p>Barker B. M., O’Connell R. F., 1975, Phys. Rev. D, 12, 329</p> <p>Bertotti B., Farinella P., Vokrouhlický D., 2003, Physics of the Solar System. Kluwer</p> <p>Brumberg V. A., 1991, Essential Relativistic Celestial Mechanics. Adam Hilger</p> <p>Carter B., 1971, Phys. Rev. Lett., 26, 331</p> | <p>Cui Y., Hada K., Kawashima T., et al., 2023, Nature, 621, 711</p> <p>Cui Y., Lin W., 2024, arXiv e-prints, arXiv:2410.10965</p> <p>Doeleman S. S., Fish V. L., Schenck D. E., et al., 2012, Science, 338, 355</p> <p>Dokuchaev V. I., 2023, Astronomy, 2, 141</p> <p>Feng J., Wu Q., 2017, Mon. Not. Roy. Astron. Soc., 470, 612</p> <p>Garofalo D., 2020, Ann. Phys.–Berlin, 532, 1900480</p> <p>Goldstein H., 1980, Classical Mechanics. Second Edition. Addison Wesley</p> |
|--|--|

- Iorio L., 2024a, General Post-Newtonian Orbital Effects From Earth's Satellites to the Galactic Center. Cambridge University Press
- Iorio L., 2024b, arXiv e-prints, arXiv:2411.08686
- Israel W., 1967, Phys. Rev., 164, 1776
- Kerr R. P., 1963, Phys. Rev. Lett., 11, 237
- Kissler-Patig M., Gebhardt K., 1998, Astron J., 116, 2237
- Kopeikin S. M., Efroimsky M., Kaplan G., 2011, Relativistic Celestial Mechanics of the Solar System. Wiley
- Li Y.-R., Yuan Y.-F., Wang J.-M., et al., 2009, Astrophys. J., 699, 513
- Liska M., Hesp C., Tchekhovskoy A., et al., 2018, Mon. Not. Roy. Astron. Soc., 474, L81
- McKinney J., Tchekhovskoy A., Blandford R. D., 2013, Science, 339, 49
- Meng X.-C., Wang C.-H., Wei S.-W., 2024, arXiv e-prints, arXiv:2411.07481
- Murray C. D., Dermott S. F., 1999, Solar System Dynamics. Cambridge University Press
- Nemmen R., 2019, Astrophys. J. Lett., 880, L26
- Newman E. T., Couch E., Chinnapared K., et al., 1965, J. Math. Phys., 6, 918
- Newman E. T., Janis A. I., 1965, J. Math. Phys., 6, 915
- Nokhrina E. E., Gurvits L. I., Beskin V. S., et al., 2019, Mon. Not. Roy. Astron. Soc., 489, 1197
- Penrose R., 1999, J. Astrophys. Astron., 20, 233
- Penrose R., 2002, Gen. Relativ. Gravit., 7, 1141
- Poisson E., Will C. M., 2014, Gravity. Newtonian, Post-Newtonian, Relativistic. Cambridge University Press
- Robinson D. C., 1975, Phys. Rev. Lett., 34, 905
- Roy A. E., 2005, Orbital Motion. Fourth Edition. IOP Publishing
- Shapiro S. L., Teukolsky S. A., 1986, Black Holes, White Dwarfs and Neutron Stars: The Physics of Compact Objects. Wiley
- Shapiro S. L., Teukolsky S. A., 1991, Phys. Rev. Lett., 66, 994
- Sob'yanin D. N., 2018, Mon. Not. Roy. Astron. Soc., 479, L65
- Soffel M. H., 1989, Relativity in Astrometry, Celestial Mechanics and Geodesy. Springer
- Soffel M. H., Han W.-B., 2019, Applied General Relativity, Astronomy and Astrophysics Library. Springer
- Taff L. G., 1985, Celestial Mechanics: A Computational Guide for the Practitioner. Wiley
- Tamburini F., Thidé B., Della Valle M., 2020, Mon. Not. Roy. Astron. Soc., 492, L22
- Teukolsky S. A., 2015, Class. Quantum Gravit., 32, 124006
- Wang J.-M., Li Y.-R., Wang J.-C., Zhang S., 2008, Astrophys. J. Lett., 676, L109
- Yodzis P., Seifert H.-J., Müller Zum Hagen H., 1973, Communications in Mathematical Physics, 34, 135